Cytogenetic Instability in Ovarian Epithelial Cells from Women at Risk of Ovarian Cancer

Tanja Pejovic,[1,2,3] Jane E. Yates,[3] Hong Y. Liu,[1] Laura E. Hays,[3] Yassmine Akkari,[4] Yumi Torimaru,[4] Winifred Keeble,[3] R. Keaney Rathbun,[3] William H. Rodgers,[6] Allen E. Bale,[7] Najim Ameziane,[8] C. Michael Zwaan,[10] Abdellatif Errami,[9] Philippe Thuillier,[3] Fabio Cappuccini,[1,2] Susan B. Olson,[4] Joanna M. Cain,[1,2] and Grover C. Bagby, Jr.[3,4,5]

[1]Department of Obstetrics and Gynecology, [2]Center for Women's Health, [3]Oregon Health & Science University Cancer Institute, and [4]Department of Medicine and Molecular and Medical Genetics, Oregon Health & Science University; [5]Northwest Veterans Affairs Cancer Research Center, Portland Veterans Affairs Medical Center, Portland, Oregon; [6]Department of Pathology, University of Maryland, Baltimore, Maryland; [7]Department of Genetics, Yale University School of Medicine, New Haven, Connecticut; [8]Department of Clinical and Human Genetics, Vrije University Medical Center; [9]MRC-Holland B.V., Amsterdam, the Netherlands; and [10]Department of Pediatric Oncology, Erasmus Medical Center/Sophia Children's Hospital, Rotterdam, the Netherlands

Abstract

Fanconi anemia is an inherited cancer predisposition disease characterized by cytogenetic and cellular hypersensitivity to cross-linking agents. Seeking evidence of Fanconi anemia protein dysfunction in women at risk of ovarian cancer, we screened ovarian surface epithelial cells from 25 primary cultures established from 22 patients using cross-linker hypersensitivity assays. Samples were obtained from (*a*) women at high risk for ovarian cancer with histologically normal ovaries, (*b*) ovarian cancer patients, and (*c*) a control group with no family history of breast or ovarian cancer. In chromosomal breakage assays, all control cells were mitomycin C (MMC) resistant, but eight samples (five of the six high-risk and three of the eight ovarian cancer) were hypersensitive. Lymphocytes from all eight patients were MMC resistant. Only one of the eight patients had a *BRCA1* germ-line mutation and none had *BRCA2* mutations, but FANCD2 was reduced in five of the eight. Ectopic expression of normal *FANCD2* cDNA increased FANCD2 protein and induced MMC resistance in both hypersensitive lines tested. No *FANCD2* coding region or promoter mutations were found, and there was no genomic loss or promoter methylation in any Fanconi anemia genes. Therefore, in high-risk women with no *BRCA1* or *BRCA2* mutations, tissue-restricted hypersensitivity to cross-linking agents is a frequent finding, and chromosomal breakage responses to MMC may be a sensitive screening strategy because cytogenetic instability identified in this way antedates the onset of carcinoma. Inherited mutations that result in tissue-specific *FANCD2* gene suppression may represent a cause of familial ovarian cancer. (Cancer Res 2006; 66(18): 9017-25)

Introduction

Ovarian carcinomas, thought to arise from the ovarian surface epithelium (OSE; ref. 1), often show signs of genetic instability, including recurrent nonrandom chromosomal abnormalities (2), oncogene activation by translocations or point mutations (3–7), and inactivation of tumor suppressor genes, including *TP53, WT1, BRCA1*, and *NOEY2* (8–12). The causes of genetic instability in these cells (independent of *BRCA1* and *BRCA2* mutations) have not been identified, and it is not at all clear whether instability is an early or late event in multistep carcinogenesis.

Studies on the pathogenesis of rare human chromosomal breakage syndromes, such as Fanconi anemia, have helped define the molecular basis of the linkage of defective DNA damage responses and cancer risk. Indeed, for Fanconi anemia, there is clear biochemical evidence that the Fanconi anemia gene products integrate with BRCA1 and BRCA2 function. Fanconi anemia is a rare genetic disorder characterized by skeletal anomalies, progressive bone marrow failure, cancer susceptibility, and cellular hypersensitivity to DNA cross-linking agents. Eleven Fanconi anemia genes have been identified to date: *FANCA, FANCB, FANCC, FANCD1, FANCD2, FANCE, FANCF, FANCG, FANCJ, FANCL*, and *FANCM* (13–15). Of these, *FANCA, FANCB, FANCC, FANCE, FANCF, FANCG, FANCL*, and *FANCM* form a nuclear core complex. Although the functional scope of this complex has not been fully defined, it is clear that it must be completely intact for it to facilitate the monoubiquitination of the downstream FANCD2 protein (16), a change that permits the protein to colocalize with BRCA1, BRCA2, and RAD51 in damage-induced nuclear foci (17, 18). This monoubiquitinated form (FANCD2-L; 162 kDa) can be readily identified and distinguished from the nonubiquitinated form (FANCD2-S; 155 kDa) by immunoblotting (19). Therefore, the mitomycin C (MMC) hypersensitive phenotype, which can be caused either by failure of cells to ubiquitinate FANCD2 or by loss of FANCD2 expression, can be readily screened in this way.

Three lines of evidence suggest that the Fanconi anemia pathway may be linked with ovarian carcinogenesis. First, *BRCA2* has been identified as the Fanconi anemia gene *FANCD1* (20). Consequently, whereas heterozygotes for *BRCA2* mutations have a high risk of tissue-specific epithelial cancers, homozygotes have Fanconi anemia. Second, an increased prevalence of epithelial cancers, including ovarian malignancies, has been observed in Fancd2 nullizygous mice (21). Finally, Taniguchi et al. (22) described functionally significant silencing of *FANCF* in ovarian cancer cell lines and in primary ovarian cancers through promoter hypermethylation, although whether epigenetic silencing of this gene occurs early or late in carcinogenesis is unclear.

In this study, we sought to identify abnormalities in cross-linking agent responses and Fanconi anemia protein function in ovarian

epithelial cells from women at high risk of ovarian cancer (histologically normal ovaries removed prophylactically from women with personal or family history of breast and/or ovarian cancer). We report here that the majority of samples from high-risk women and nearly half of ovarian cancer samples exhibited MMC-induced cytogenetic instability and that lymphocytes from none of these patients exhibited such genetic instability. Only one of these patients was a *BRCA1* heterozygote, and none showed *BRCA2* mutations. A significant proportion of the primary epithelial cells from these patients was shown to have low expression of *FANCD2* mRNA and FANCD2 protein. In two such patients studied in further detail, the expression of FANCD2 protein was suppressed in ovarian epithelial cells but not in lymphocytes.

Materials and Methods

Patients and Procurement of Tissue

Ovarian samples were collected intraoperatively after having obtained signed informed consent from women undergoing primary surgery for benign gynecologic disease, from ovarian cancer patients undergoing an initial staging/debulking procedure, and from women at high risk for ovarian cancer undergoing prophylactic oophorectomy (Table 1). Patients at high risk for ovarian cancer were defined as women with (*a*) a family history of one or more first-degree relatives diagnosed with ovarian cancer before the age of 50 years, (*b*) a family history of one first-degree relative with ovarian cancer and one or more first- or second-degree relatives diagnosed with breast or ovarian cancer, or (*c*) a personal history of breast cancer and one or more first- or second-degree relatives diagnosed with breast or ovarian cancer (23). None of the patients had received any cytotoxic chemotherapy or radiation before surgery.

Cell Culture

A total of 25 samples were obtained, including normal ovarian tissue (11 samples from 9 patients), high-risk ovarian tissue (6 samples from 5 patients), and ovarian cancer samples (8 samples from 8 patients). The ovarian cells were scraped from the ovarian surface and enzymatically disaggregated with collagenase I (Life Technologies-Invitrogen, Grand Island, NY) for 4 hours. The cells were washed in RPMI 1640 (Life Technologies-Invitrogen) and plated in 25 cm^2 flasks coated with collagen in RPMI 1640 supplemented with 20% FCS (Hyclone, Logan, UT), 10 μg/mL insulin (Sigma, St. Louis, MO), and 10 ng/mL epidermal growth factor (R&D Systems, Minneapolis, MN). Ovarian cells were transformed by transduction with a retrovirus expressing SV40 large T antigen (24). The cell line ψ-2/U195, which produces this retrovirus, was kindly provided by Dr. Roger Cone (Oregon Health & Science University, Portland, OR; ref. 25). SV40-transformed ovarian epithelial cells were transduced with pMMP retroviral vectors containing full-length *FANCD2* cDNA (26, 27). The cell line AM12/RVD2 (kindly provided by Markus Grompe, Oregon Health & Science University) stably produces the pMMPpuro/FANCD2 retrovirus.

Lymphocytes were isolated from peripheral blood using Ficoll-Paque PLUS (Amersham Biosciences, Piscataway, NJ) and then stimulated with 1% phytohemagglutinin (PHA) with and without MMC for 4 days before harvest. Harvested lymphocytes were used to prepare protein lysates and RNA and for chromosomal breakage analyses (below).

The ovarian cancer cell lines PA1 and OVCAR-3 and the cervical epithelial cell line HeLa (American Type Culture Collection, Manassas, VA) were also used for p53 studies. In experiments designed to quantify the function of p53, RNA was obtained from these three cell types and the primary cells OV-HR3, OV-HR4L, and OV-HR5R (Table 1) before and 18 hours after exposure to 20 J/m^2 UV radiation. RNA was used in real-time reverse transcription-PCR (RT-PCR) to detect fold changes in three p53-responsive genes: *p21, Noxa,* and *Puma*.

MMC Sensitivity Assay

Cell survival assays. Epithelial cells (6×10^3) were incubated with various concentrations of MMC (range, 0-250 nmol/L; Sigma) in 12-well plates in RPMI 1640 with 15% FCS, 100 units/mL penicillin/streptomycin, and 2 mmol/L L-glutamine. After a 5-day incubation, cells in the monolayer were trypsinized and live cells were counted using the trypan blue dye exclusion method. Cell viability was expressed as percentage of trypan blue–excluding (viable) cells in the MMC-treated sample relative to that of the untreated control sample. Each sample was tested in triplicate.

Chromosomal breakage analysis. For breakage studies, cell cultures were incubated with 40 ng/mL MMC and 200 ng/mL diepoxybutane (DEB) at 37°C for 48 hours in RPMI 1640 in the dark. These cultures were then harvested after a 2-hour exposure to 0.25 μg/mL colcemid (Sigma). Following a 10-minute treatment with hypotonic solution (0.075 mol/L KCl, 5% FCS), the cells were fixed with a 3:1 mixture of methanol-acetic acid. Slides were stained with Wright's stain and scored for chromosomal breaks and radial forms.

Immunoblots

Cells (1×10^6) were treated with or without 50 nmol/L MMC for 48 hours. Whole-cell extracts were prepared in lysis buffer [50 mmol/L Tris-HCl (pH 7.4), 150 mmol/L NaCl, 1% NP40, 0.1% sodium deoxycholate, 4 mmol/L EDTA] supplemented with protease inhibitors (1 μg/mL leupeptin and pepstatin A, 2 mg/mL aprotinin, and 1 mmol/L phenylmethylsulfonyl fluoride) and phosphatase inhibitors (2 mmol/L sodium orthovanadate and 10 mmol/L NaF). Cell lysates were separated by SDS-PAGE and immunoblotted as described elsewhere (28). Primary antibodies were as follows: monoclonals anti-FANCD2 (diluted 1:200; Santa Cruz Biotechnology, Santa Cruz, CA) and anti-α-tubulin (diluted 1:500; Sigma) and polyclonals anti-FANCA (diluted 1:100; R&D Systems), anti-FANCC (diluted 1:150; R&D Systems), anti-p53 (diluted 1:1,000; Calbiochem, San Diego, CA), and anti-β-actin (diluted 1:500; Santa Cruz Biotechnology). Secondary antibodies (1:10,000 dilution) were horseradish peroxidase–conjugated goat anti-mouse or goat anti-rabbit antibody (Bio-Rad, Hercules, CA).

Amplification and Sequencing of *FANCD2* mRNA and DNA

Total RNA was prepared from 0.5×10^6 to 5×10^6 cells using the RNeasy Mini kit (Qiagen, Inc., Valencia, CA). First-strand cDNA was synthesized using 2.0 μg RNA, 200 ng random hexamers (Invitrogen, Carlsbad, CA), and SuperScript III reverse transcriptase (Invitrogen) according to the manufacturer's instructions. PCR of full-length *FANCD2* coding sequences was then done with 2.0 μL cDNA, primers Xho-D2-1 (5′-AGCTCGAGAT-GGTTTCCAAAAGAAGACTGTCAAAA-3′) and Not-D2-4411 (5′-ATTGCGGC-CGCCTAATCAGAGTCATCATAACTCTC-3′), and PfuUltra polymerase (Stratagene, La Jolla, CA). PCR products were cloned using the pCR-Blunt II-TOPO system (Invitrogen), and cDNA inserts from individual clones were sequenced with the use of the BigDye Terminator version 3.1 Cycle Sequencing kit and an ABI 3100 Genetic Analyzer (Applied Biosystems, Foster City, CA). Sequencing primers were chosen with a 200 bp reading overlap to insure full coverage. A cDNA insert containing the ex16-18del splice variant was subcloned into the retroviral vector pLXSN (a gift of A.D. Miller, Fred Hutchinson Cancer Research Center, Seattle, WA). The method used for retroviral vector production and transduction has been described previously (28). PCR amplification to confirm the presence of the ex16-18del splice variant was done on 2.0 μL cDNA using primers designed to bind within exons 14 and 20 of *FANCD2* (upstream primer sequence, 5′-CAAG-AAAGCAGCGGTCAGAG-3′; downstream primer sequence, 5′-ACAGCAC-CAATAATCCCAATG-3′). PCR products were electrophoresed on a 1% agarose gel.

Genomic DNA was isolated from ovarian cells using the QIAamp DNA Mini kit (Qiagen). *FANCD2* exon-intron boundaries were amplified by PCR using 50 ng genomic DNA as template and one unit Taq DNA polymerase (Promega, Madison, WI). PCR products were sequenced as outlined above. The *FANCD2* promoter was amplified using 100 ng genomic DNA as template and Phusion High-Fidelity DNA Polymerase (New England Biolabs, Ipswich, MA) according to the manufacturer's instructions. Primers were designed to bind just within the 5′-untranslated region of *FANCD2* (5′-TACTCACCGAGAAGCCGTCG-3′) and ∼1.2 kb upstream (5′-CTAC-CATGTGCCTTGCACTCTG-3′). PCR products were sequenced as above, and those results were confirmed by sequencing the opposite strand.

Table 1. Clinicopathologic and molecular characteristics of 22 cases studied

Cases	Age	Pathology	Radials (%)		FANCD2 expression (OSE)
			OSE	PBML	
			MMC/DEB	MMC/DEB	
Normal					
OV-NL1	62	ROV: no abnormalities	0/0	ND	Normal
		LOV: endometriosis			
OV-NL2	51	Uterine fibroids. Normal ovaries	0/0	ND	Normal
OV-NL3	40	Metrorrhagia. Normal ovaries	2/0	0/0	Normal
OV-NL4	54	LOV: no abnormalities	4/1	ND	Normal
		ROV: benign serous cystadenoma			
OV-NL5	68	LOV: fibroma	1/1	ND	Normal
		ROV: no abnormalities			
OV-NL6L	43	CIN III. Normal ovaries	0/0	0/ND	Normal
OV-NL6R			0/0	0/ND	
OV-NL7	54	LOV: benign serous cystadenoma	1/2	ND	Normal
		ROV: no abnormalities			
OV-NL8	55	Uterine polyp. Normal ovaries	3/3	ND	Normal
OV-NL9L	48	Uterine fibroid. Normal ovaries	0/0	0/0	Normal
OV-NL9R			0/0	0/0	
High risk					
OV-HR1	30	No evidence of multifocal surface papillomatosis, pseudostratification, or activity of the epithelium or ovarian stroma in any high risk sample	10/14	0/0	Normal
OV-HR2	71		50/64	0/0	Reduced
OV-HR3	43		64/55	1/0	Normal
OV-HR4L	35		66/50	0/0	Reduced
OV-HR5L	71		47/20	0/1	Reduced
OV-HR5R			30/12	0/0	Reduced
Carcinoma					
OV-CA1	72	Poorly differentiated serous carcinoma, stage IIIC	14/16	2/0	Normal
OV-CA2	52	Poorly differentiated serous carcinoma, stage IV	12/10	1/0	Normal
OV-CA3	63	Moderately differentiated serous carcinoma, stage IIIB	16/14	1/1	Normal
OV-CA4	70	Poorly differentiated serous carcinoma, stage IIIC	70/48	4/2	Reduced
OV-CA5	54	Poorly differentiated serous carcinoma, stage IIIC	12/2	2/0	Normal
OV-CA6	73	Poorly differentiated serous carcinoma, stage IV	66/ND	1/1	Normal
OV-CA7	58	Poorly differentiated serous carcinoma, stage IIIC	0/ND	0/1	Normal
OV-CA8	62	Poorly differentiated serous carcinoma, stage IIIC	33/ND	3/1	Normal

Abbreviations: LOV, left ovary; ROV, right ovary; CIN III, cervical intraepithelial dysplasia III; ND, not determined.

Real-time RT-PCR

Real-time PCR was done on triplicate 50 ng aliquots of each cDNA sample (prepared above) using Taqman Universal PCR Master Mix and an ABI PRISM 7000 Sequence Detection System (Applied Biosystems) according to the manufacturer's instructions. All reactions were done in multiplex format with a VIC/MGB-labeled, primer-limited eukaryotic 18S rRNA internal standard probe (Applied Biosystems). After PCR, threshold cycles were determined for each gene and then values were normalized using the threshold cycles of the 18S rRNA standard. The mean normalized value of each triplicate was determined, and fold change was calculated using the $\Delta\Delta C_t$ method (29). Predesigned primer and probe sets for 20 of the genes were purchased as Taqman Gene Expression Assays from Applied Biosystems and are as follows (assay ID in parentheses): *ATR* (Hs00169878_m1), *BID* (Hs00609630_m1), *BLM* (Hs00172060_m1), *DCLRE1C* (Hs00223928_m1), *ERCC1* (Hs00157415), *ERCC4* (Hs00193342_m1), *H2AFX* (Hs00266783_s1), *HTATIP* (Hs00197310_m1), *MRE11A* (Hs00271551_m1), *NBN* (Hs00159537_m1), *RAD51* (Hs00153418_m1), *RAD54L* (Hs00269177_m1), *REV3L* (Hs00161301_m1),

TP53 (Hs00153349), *XRCC2* (Hs00538799_m1), *XRCC3* (Hs00193725_m1), *FANCL* (Hs01015742_m1), *CDKN1A* (p21; Hs00355782_m1), *BBC3* (Puma; Hs00248075_m1), and *PMAIP1* (Noxa; Hs00560402_m1). The remainder of the primer/probe sets was designed with the aid of ABI PRISM Primer Express software version 2.0.0 (Applied Biosystems). Sequences are listed in Supplementary Table S1. Primers for these sets were synthesized by Integrated DNA Technologies (Coralville, IA), whereas 6-FAM/MGB probes were made by Applied Biosystems.

DNA Copy Number Analysis of Fanconi Anemia and Other Chromosome Instability Genes

The oligonucleotide array comparative genomic hybridization (CGH) method used here has been described previously (30). Briefly, a whole-genome array with a 6 kb median probe spacing was used to map single and multiple copy number genomic alterations. Oligonucleotide probes ($T_m = 76°C$, 45-85 nucleotides in length) were tiled through genic and intergenic regions. Genomic DNA extracted from primary OSE cells was fragmented to 500 to 2,000 bp by sonication and then labeled with either

5′-Cy3 or 5′-Cy5 dye according to the method of Selzer et al. (30). Differentially labeled test and reference sample (15 μg of each) were combined in NimbleGen Hybridization Buffer (NimbleGen Systems, Inc., Madison, WI), denatured at 95°C for 5 minutes, and then hybridized for 18 hours at 42°C. The arrays were washed with NimbleGen Wash Buffer System and dried by centrifugation. The reference sample was a pool of DNA (extracted from peripheral blood lymphocytes) from six male individuals (Promega). Arrays were scanned at 5 μm resolution using a GenePix 4000B scanner (Axon Instruments, Molecular Devices Corp., Sunnyvale, CA). Data were extracted from scanned images using NimbleScan 2.0 extraction software (NimbleGen Systems). Data analysis included normalization of signal intensities of the test sample versus reference sample. The $\log_2$ ratios were averaged with a fixed window size corresponding to 5×, 10×, and 20× the median probe spacing. Unaveraged and window-averaged $\log_2$ ratios were used as input to the DNA copy package of the Bioconductor software to produce the final segmentations (31) that demarcate DNA copy number changes.

Promoter Methylation Analysis of Fanconi Anemia Genes

Probes to detect methylated promoters by the method of methylation specific-multiplex ligation-dependent probe amplification (MS-MLPA) were designed as described previously (32), except that the promoter sequences detected by these probes contain a recognition site for *Hha*I methylation-specific restriction enzyme. The kit used for this study contained probes that were targeted against the promoter regions of all the identified Fanconi anemia genes (*FANCA, FANCB, FANCC, FANCD1, FANCD2, FANCE, FANCF, FANCG, FANCJ, FANCL*, and *FANCM*). Probe sequences are listed in Supplementary Table S2. Each Fanconi anemia gene was represented by two MS-MLPA probes, except *FANCA* and *FANCG* (one probe each) and *FANCF* (three probes). The MLPA reagents were obtained from MRC-Holland (Amsterdam, the Netherlands). Approximately 25 ng of genomic DNA in 5 μL of TE buffer [10 mmol/L Tris-HCl (pH 8.5), 1 mmol/L EDTA] were denatured for 10 minutes at 98°C. SALSA MLPA buffer (1.5 μL) and MS-MLPA probes (1 fmol each and 1.5 μL volume) were then added and,

after incubation for 1 minute at 95°C, were allowed to hybridize to their respective targets for 16 hours at 60°C. After hybridization, the mixture was diluted at room temperature with H_2O and 3 μL ligase buffer A to a final volume of 20 μL and then equally divided in two tubes. While at 49°C, a mixture of 0.25 μL Ligase-65 (MRC-Holland), 5 units *Hha*I (Invitrogen), and 1.5 μL ligase buffer B in a total volume of 10 μL was added to one tube. The second tube was treated identically, except that the *Hha*I enzyme was replaced with H_2O. Simultaneous ligation and digestion was then done by incubation for 30 minutes at 49°C followed by 5 minutes of heat inactivation of the enzymes at 98°C. The ligation products were PCR amplified by the addition of 5 μL of this ligation mixture to 20 μL PCR mixture containing PCR buffer, deoxynucleotide triphosphates, SALSA polymerase, and PCR primers (one unlabeled and one D4 labeled) at 60°C as described by Schouten et al. (33). PCR products were run on an ABI PRISM 310 Genetic Analyzer (Applied Biosystems) and analyzed using GeneScan analysis software version 3.7 (Applied Biosystems).

Results

MMC-induced chromosomal breakage. The reference range of MMC- and DEB-induced chromosome radial formation has been well established using fibroblasts and lymphoid cells, but the range of normal responses has not been defined for primary cultures of normal ovarian epithelial cells. We found that epithelial cells from all normal ovarian samples showed levels of MMC- and DEB-induced radial formation consistent with the range defined for other well-studied normal cell types (<20% of metaphases). However, five of the six high-risk ovarian samples and three of the eight ovarian cancer samples had increased levels of chromosomal breakage and radial formation (Table 1). To rule out the unlikely possibility that all of these genetically unstable ovarian cells were from atypical patients with Fanconi anemia, peripheral
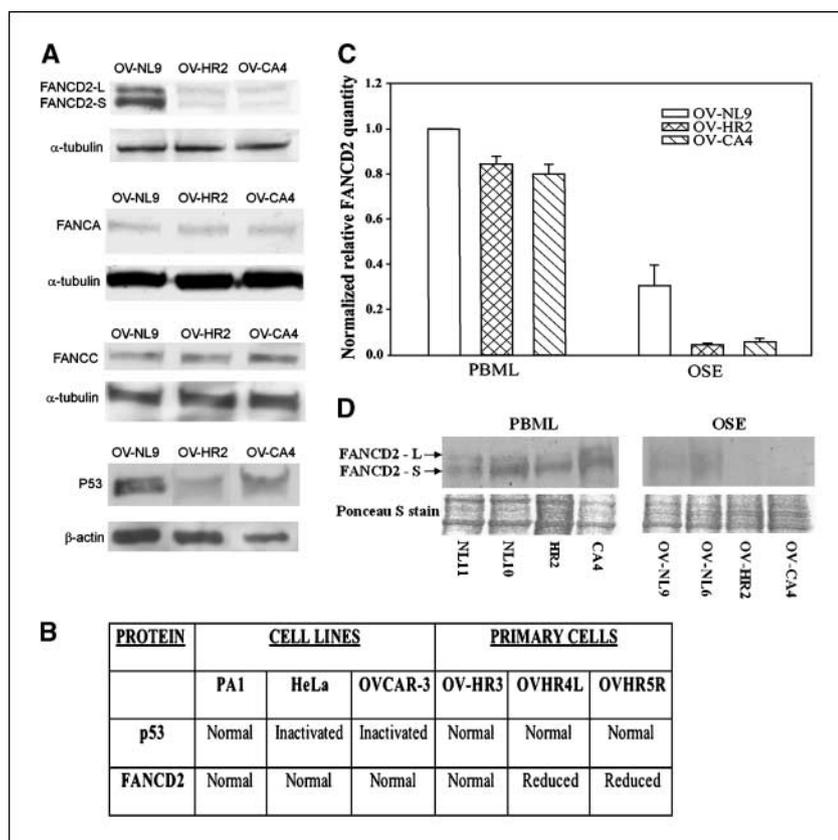

Figure 1. *A,* immunoblots of primary ovarian epithelial cells. Cells were treated with 50 nmol/L MMC for 48 hours before harvest and then immunoblotted for FANCD2, FANCA, FANCC, and p53 protein. OV-NL9 is a normal control, OV-HR2 is a high-risk sample, and OV-CA4 is an ovarian cancer sample. FANCD2-S and FANCD2-L bands are indicated. *Bottom,* α-Tubulin and β-actin loading controls. *B,* functional status of p53 was defined in six UV-irradiated (20 J/m²) cell types. Normal p53 response is defined as >1.5-fold induction of p21, Noxa, and Puma gene expression by UV radiation. In OVCAR-3 cells, p53 is inactivated by an R248Q point mutation, and in HeLa, p53 is inactivated by human papillomavirus oncogene E6. FANCD2 levels in all cells were assessed by immunoblotting. *C,* relative amounts of *FANCD2* mRNA in peripheral blood mononuclear lymphocytes (PBML) and primary OSE cells of a high-risk (OV-HR2) and ovarian cancer patient (OV-CA4). RNA from equivalent cell numbers was reverse transcribed, and *FANCD2* cDNA was amplified by Taqman real-time PCR. Each sample was measured in triplicate. *White columns,* mean expression levels in two normal individuals. *D,* PBML and OSE protein lysates immunoblotted for FANCD2 protein. *Bottom,* Ponceau S stain for total protein. *Left,* PBML from two normal controls (NL10 and NL11), a high-risk patient (HR2), and ovarian cancer patient (CA4). NL10 and NL11 are healthy patients, with no associated ovarian or other pathology. *Right,* FANCD2 expression in normal ovarian epithelial cells (OV-NL9 and OV-NL3), high-risk OSE (OV-HR2), and ovarian cancer (OV-CA4). Cells were not treated with MMC before harvest, and therefore, low levels of FANCD2 in OV-HR2 and OV-CA4 were revealed only after longer exposure of the film (data not shown).

blood lymphocytes were obtained and subjected to MMC/DEB-induced chromosomal breakage testing. None of the lymphocytes were hypersensitive to MMC or DEB (Table 1).

Fanconi anemia pathway defects identified by FANCD2 immunoblot. Having determined that both the histologically normal epithelial cells from high-risk women and the epithelial ovarian cancer cells exhibited cross-linking agent hypersensitivity, we sought to determine whether MMC/DEB sensitivity could be the result of inherited or acquired dysfunction of the proteins known to be involved in protecting the genome from damage by cross-linking agents, including those proteins that make up the Fanconi anemia core complex and other proteins with which that complex is known to interact.

All 25 primary ovarian epithelial cell cultures were treated with 50 nmol/L MMC for 48 hours and then screened for the presence of FANCD2 long (L) and short (S) forms by immunoblotting (19). Reduced levels of FANCD2 protein (both the -L and -S forms) were consistently found in four of the six high-risk and one of the three breakage-positive ovarian cancer samples. Total FANCD2 levels were never reduced in cells that were resistant to alkylating agents in the chromosomal breakage test. Two samples selected for further study, OV-HR2 from a cancer-free, high-risk patient and OV-CA4 from ovarian cancer cells, showed markedly reduced levels of FANCD2-L and FANCD2-S protein isoforms compared with normal control (Fig. 1*A*). However, other proteins involved in pathways of DNA damage response, including FANCA and FANCC, showed no such reduction in levels in the high-risk or ovarian cancer cells compared with normal control (Fig. 1*A*). Immuno-blotting with anti-p53 antibody revealed that full-length protein was present in all samples, ruling out large genomic deletions of this gene that might be expected in cells with chromosomal instability (Fig. 1*A*). Oligonucleotide array CGH experiments also ruled out p53 deletion, with no genomic loss of chromosome band 17p13.1 found. Additionally, we determined that p53 function was normal in three of our primary cells tested (OV-HR3, OV-HR4L, and OV-HR5R). As a control, we first confirmed normal p53 function (PA1 cells) or loss of function (OVCAR-3 and HeLa) previously described for these cells (34, 35) and then showed that FANCD2 levels were normal in the three lines. Thus, FANCD2 gene expression is not controlled by p53 (Fig. 1*B*). In contrast to the results in primary OSE cells, *FANCD2* mRNA (Fig. 1*C*) and protein (Fig. 1*D*) were readily detectable in PHA-stimulated peripheral blood lymphocytes from the same subjects.

To confirm that FANCD2 deficiency played a role in the genetic instability of OV-HR2 and OV-CA4 cells, we first SV40 transformed these cells and then transduced the cells with pMMP retrovirus containing the *FANCD2* cDNA. SV40-transformed OV-HR2 and OV-CA4 cells continued to show low FANCD2 protein levels compared with SV40-transformed OV-NL3 (normal) cells (Fig. 2*A*). After transduction of the *FANCD2* retrovirus into these OV-HR2 and OV-CA4 cells, normal FANCD2 levels were restored, and the cells responded normally to cross-linker exposure as shown by increased levels of FANCD2-L after treatment with MMC (Fig. 2*A*). FANCD2-deficient OV-HR2 and OV-CA4 cells show impaired survival even at low doses of MMC (LD_{50} = 5-10 nmol/L, compared with an approximate LD_{50} of 150 nmol/L in control cells; Fig. 2*B*), but survival was greatly increased after transduction of the cells with the *FANCD2* retroviral vector (LD_{50} = 100 nmol/L). Survival of OSE that had normal MMC responses in the breakage assay (OV-NL9) was not significantly enhanced by ectopic expression of FANCD2 (Fig. 2*B*). In addition, FANCD2 transduction of OV-HR2
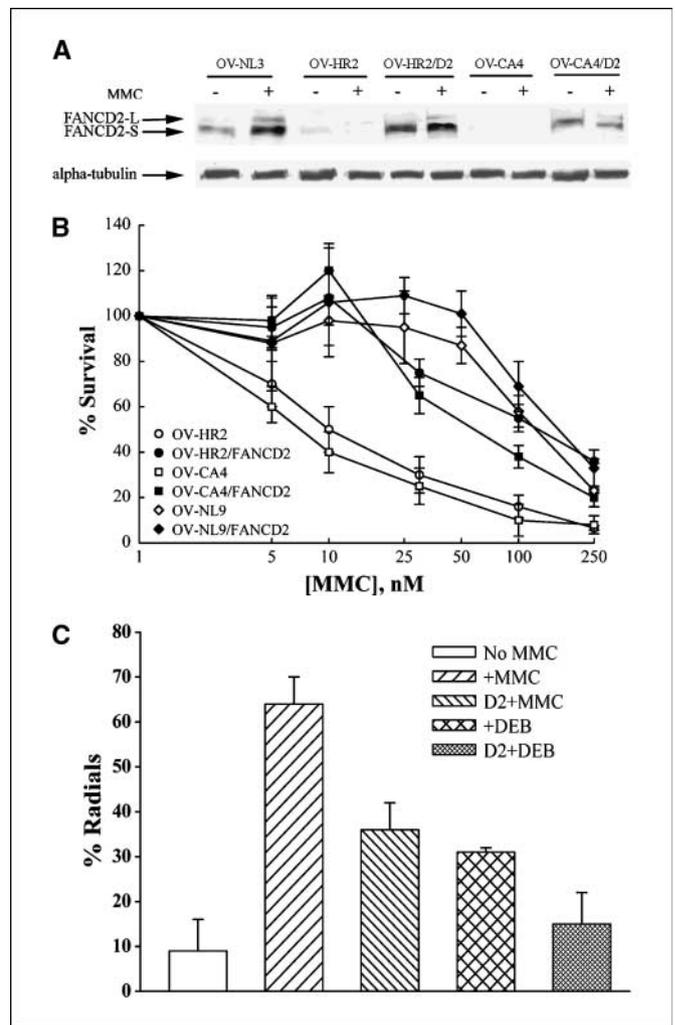

Figure 2. Restoration of FANCD2 expression and function after retroviral transduction of normal *FANCD2* cDNA. SV40-transformed ovarian epithelial high-risk cells (OV-HR2) and ovarian cancer cells (OV-CA4) were transduced with pMMP retroviral vectors containing full-length *FANCD2* cDNA. *A,* OSE cells were treated with 50 nmol/L MMC for 48 hours before harvest and immunoblotting with anti-FANCD2 antibody. FANCD2-S and FANCD2-L bands are indicated. α-Tubulin was used as a protein loading control. *B,* OSE cells (*closed symbols*) or OSE cells transduced with *FANCD2* cDNA (*open symbols*) were treated for 5 days with MMC (0-250 nmol/L), and cell survival was measured by the trypan blue dye exclusion method. *Points,* mean of three biological replicates; *bars,* SD. OV-NL9 is a normal control sample. *C,* FANCD2 complementation partially corrects MMC-induced radial formation in high-risk (OV-HR2) ovarian epithelium. FANCD2-deficient OSE (*columns 1, 2,* and *4*) and FANCD2-complemented OSE (*columns 3* and *5*) were incubated with 40 ng/mL MMC or 200 ng/mL DEB for 48 hours. The percentage of radial formations out of 50 metaphases examined per case was then determined. A cutoff value of 20% was used to distinguish normal versus increased radial formation.

significantly reduced the fraction of MMC- and DEB-exposed cells bearing radial forms (Fig. 2*C*) from 64% to 36% (MMC) and 31% to 15% (DEB).

FANCD2 cDNA and promoter sequences are normal in unstable epithelial cells with low FANCD2 levels. Cloning and sequencing of the *FANCD2* cDNA samples from OV-HR2 and OV-CA4 revealed the existence of two distinct transcripts, each found in multiple clones: one, the full-length wild-type sequence and the other, a differentially spliced form showing a deletion of exons 16 to 18. Deletion of exons 16 to 18 was confirmed using RT-PCR with primers designed to bind specifically within exons 14 and

20 of *FANCD2*. PCR products were analyzed by agarose gel electrophoresis for the presence of either a wild-type fragment of 733 bp or a truncated 325 bp product corresponding to the exons 16 to 18 deleted splice form. Both wild-type and exons 16 to 18 deleted transcripts were found in ovarian tissue of OV-HR2 and OV-CA4 but were also detected in the lymphocytes from both patients. In addition, both transcripts were found in samples of normal ovarian epithelial cells and normal lymphocytes (Fig. 3*A*). Sequencing of genomic DNA from both patients from *FANCD2* exons 15 to 20 revealed no mutations of the consensus splice sites. The predicted protein from this alternatively spliced form would be 145 kDa; however, immunoblots of normal ovarian epithelial cells using an antibody targeted to the FANCD2 NH_2 terminus did not reveal the presence of a protein of this molecular weight. The ability of this splice variant either to complement a FANCD2-deficient cell or to suppress activity of wild-type FANCD2 in a normal cell was also explored. Ectopic expression of a FANC-D2ex16-18del cDNA in the PD20 fibroblast line from a FANCD2-deficient Fanconi anemia patient did not correct the MMC hypersensitivity of these cells in contrast to expression of a wild-type FANCD2 construct (Fig. 3*B*). In addition, overexpression of the splice variant in the normal lymphoblast cell line JY had no effect on the survival of these cells after MMC exposure (Fig. 3*C*), suggesting that it does not act as a dominant-negative protein. To our knowledge, this is the first report of this alternatively spliced form of *FANCD2* mRNA.

The *FANCD2* promoter regions from patients OV-HR2 and OV-CA4 were also examined for mutations. Approximately 1.2 kb of promoter sequences proximal to the transcription start site were amplified and sequenced. No mutations or polymorphisms were found that could distinguish the low FANCD2 samples from wild-type consensus sequence.

Real-time RT-PCR. To determine whether other genes known to play a role in protection of cells from cross-linking agents might be involved in the increased sensitivity of ovarian epithelial cells to MMC, real-time RT-PCR was used to quantify transcripts of those genes (Table 2). Using reverse-transcribed mRNA prepared from the high-risk OV-HR2 and cancer OV-CA4 primary OSE cells, relative expression levels of 24 genes were measured using gene-specific Taqman probes. Expression levels were normalized to an internal 18S rRNA control and then compared with the mean level from two normal control samples to determine the fold change. Only *FANCD2* was consistently lower in both patient samples compared with normal controls (6.4-fold lower in OV-HR2 and 5.0-fold lower in OV-CA4).

No genetic loss of *FANCD2* in epithelial cells with low FANCD2 expression. CGH analysis on whole-genome oligonucleotide arrays was done on samples OV-HR2 and OV-CA4 by the method of Selzer et al. (30). In both samples, the *FANCD2* gene locus was intact, with no gain or loss of 3p25.3 sequences at the array CGH resolution that was tested (6 kb median probe spacing or 12 probes for the ∼75 kb *FANCD2* gene). Similarly, there were no amplifications or deletions of sequences of the same 7 Fanconi anemia genes and 15 DNA damage response genes that were also analyzed by real-time PCR (see Table 2 for list). However, as expected, other genomic losses were identified in these transformed cells (Table 3).

Methylation state analysis. To determine whether epigenetic silencing by promoter methylation could account for low levels of FANCD2 protein, the putative *FANCD2* promoter, as well as all other Fanconi anemia gene promoters, was analyzed by MS-MLPA (32). Probes to 5′ CpG islands were designed to include a *Hha*I methylation-specific restriction site within the detected sequence. On digestion with *Hha*I, probes with a methylated recognition sequence generate a signal. If the CpG site is unmethylated, the genomic DNA/MS-MLPA probe complex is digested, preventing exponential amplification and signal detection during fragment analysis. Two probes were designed for the promoters of Fanconi anemia genes *FANCB, FANCC, FANCD1, FANCD2, FANCE, FANCJ, FANCL*, and *FANCM*. One probe each was used for *FANCA* and *FANCG*, and three probes were used for *FANCF* (Supplementary Table S1). Analyses of the products of the MS-MLPA reactions showed no methylation at any promoter tested (Supplementary Fig. S1).
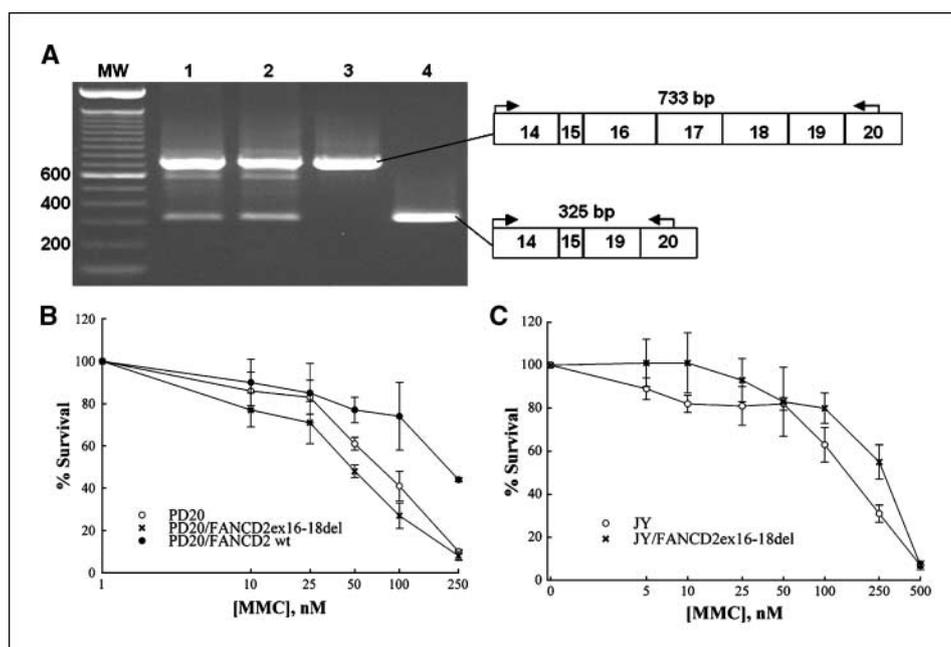

Figure 3. FANCD2ex16-18del cDNA is nonfunctional. *A,* gel electrophoresis of RT-PCR products from normal PBML (*lane 1*) or normal ovarian epithelium (*lane 2*). Amplification controls were a plasmid template containing the wild-type *FANCD2* cDNA (*lane 3*) or a plasmid template containing the cloned *FANCD2*ex16-18del splice form (*lane 4*). *Right,* exon structure of highlighted PCR products. *Arrows,* PCR primer binding sites. *Numbered boxes,* exons; *number above boxes,* predicted amplimer size. *B,* PD20 human fibroblasts were transduced with a pLXSN retrovirus expressing either wild-type FANCD2 or the FANCD2ex16-18del form. Cell survival was measured by the trypan blue exclusion method as in Fig. 2*B*. *C,* JY normal human lymphoblasts were transduced with the FANCD2ex16-18del retrovirus, and cell survival was measured as above.

Table 2. Relative mRNA levels of DNA repair and Fanconi anemia genes

Gene symbol	Gene name	OV-HR2		OV-CA4	
		Fold change, *n* (range)	Call	Fold change, *n* (range)	Call
ATR	Ataxia telangiectasia, Rad3-related	1.9 (1.7-2.1)	UP*	2.1 (1.7-2.5)	DN [†]
BID	BH3 interacting domain death agonist	1.5 (1.3-1.8)	UP	2.7 (2.2-3.3)	DN
BLM	Bloom syndrome	1.3 (1.1-1.5)	DN	4.0 (3.6-4.5)	DN
DCLRE1C	DNA cross-link repair 1C (PSO2 homologue, *Saccharomyces cerevisiae*)	1.3 (1.3-1.4)	DN	1.6 (1.4-1.8)	DN
ERCC1	Excision repair cross-complementing rodent repair deficiency 1	1.2 (1.1-1.3)	DN	1.3 (0.9-1.9)	DN
ERCC4	Excision repair cross-complementing rodent repair deficiency 2	2.0 (1.3-2.8)	UP	1.3 (1.1-1.5)	DN
H2AFX	H2A histone family, member X	2.5 (2.0-3.2)	UP	1.2 (1.0-1.5)	UP
HTATIP	HIV-1 Tat interactive protein, 60 kDa	1.0 (0.9-1.1)	—[‡]	1.1 (0.8-1.5)	—
MRE11A	Mitotic recombination 11	1.0 (0.7-1.5)	—	1.1 (0.9-1.3)	—
NBN	Nibrin, p95 protein of MRE11/RAD50 complex	1.1 (1.0-1.2)	—	1.0 (0.8-1.3)	—
RAD51	RAD51 homologue	1.4 (1.0-1.8)	DN	2.3 (1.8-3.0)	DN
RAD54L	RAD54-like (*S. cerevisiae*)	1.8 (1.5-2.1)	DN	1.6 (1.3-1.9)	DN
REV3L	REV3-like, catalytic subunit of DNA polymerase ζ (yeast)	1.9 (1.5-2.3)	UP	2.2 (1.5-3.1)	DN
TP53	Tumor protein p53	1.15 down (1.10-1.20)	—	1.16 up (1.13-1.20)	—
XRCC2	X-ray repair complementing defective repair in CHO cells 2	1.1 (0.9-1.3)	—	1.0 (0.6-1.8)	—
XRCC3	X-ray repair complementing defective repair in CHO cells 3	1.5 (1.3-1.9)	DN	1.1 (0.8-1.4)	—
FANCA	Fanconi anemia complementation group A	1.4 (1.1-1.9)	DN	1.1 (0.9-1.3)	—
FANCC	Fanconi anemia complementation group C	1.0 (0.6-1.6)	—	1.2 (0.7-2.3)	DN
FANCD2	Fanconi anemia complementation group D2	6.4 (4.6-6.9)	DN	5.0 (4.1-6.6)	DN
FANCE	Fanconi anemia complementation group E	1.6 (1.1-1.8)	DN	1.1 (1.0-1.2)	—
FANCF	Fanconi anemia complementation group F	1.9 (1.1-3.2)	UP	1.2 (0.7-2.2)	UP
FANCG	Fanconi anemia complementation group G	1.4 (1.1-1.8)	DN	3.1 (2.5-3.7)	DN
FANCL	Fanconi anemia complementation group L	1.9 (1.8-2.1)	DN	1.8 (1.1-3.0)	DN
FANCM	Fanconi anemia complementation group M	2.3 (2.2-2.3)	DN	1.9 (1.5-2.4)	DN

*An increase of 1.2-fold or more of the indicated mRNA in patient sample compared with normal control.

[†] A decrease of 1.2-fold or more in patient sample compared with normal control.

[‡] No difference in mRNA level between patient and normal control.

Discussion

Ovarian cancer is believed to arise through a series of acquired genetic changes that sequentially transform normal primitive mesothelial cells of the ovarian surface. A small percentage of ovarian cancers (5-10%) are thought to be due to inherited mutations of *BRCA1* and *BRCA2* genes and other as yet unidentified genes. However, direct mutation screening done in families with a high prevalence of ovarian cancer revealed that a significant proportion of the cases were not due to mutations in either *BRCA1* or *BRCA2* (36). The recent identification of *BRCA2* as the Fanconi anemia gene *FANCD1*, the biochemical convergence of *BRCA1/BRCA2* and Fanconi anemia pathways (16, 18, 20), and the occurrence of ovarian malignancies in Fancd2 knockout mice (21) have prompted us to speculate that *FANCD2* heterozygotes might be at higher risk of breast and/or ovarian cancer. For these reasons, we sought to determine the degree to which defects of the Fanconi anemia pathway might be important as early events in carcinogenesis.

Using the screening tool of MMC/DEB-induced chromosomal breakage (19), we examined genomic instability in ovarian epithelial cells from normal, high-risk, and ovarian cancer patients (Table 1). Histologically normal ovarian epithelial cells from five of the six high-risk women showed increased chromosomal breakage in response to MMC and DEB. All but one of the five patients tested negative for all published *BRCA1* and *BRCA2* mutation variants, and immunoblots of epithelial cell lysates revealed full-length

BRCA1 and *BRCA2* (data not shown). Therefore, mutations of neither of these genes accounted for the observed chromosomal instability. These results confirm the infrequency of *BRCA1* and *BRCA2* mutations even in women with highly suggestive family histories but also indicate that the phenotype of genomic instability in response to alkylating agents is the rule, not the exception in such cases. Of even more importance for development of more robust screening assays is our observation that cross-linking agent-induced genetic instability is detected only in ovarian epithelial cells and not in isogenic lymphocytes.

In light of these results, we hypothesized that alterations in Fanconi anemia genes may cause inherited ovarian cancer predisposition and screened all samples for aberrations in Fanconi anemia protein function. Interestingly, there was a striking decrease in FANCD2 protein levels in the majority of genetically unstable cell populations. However, function of the eight Fanconi anemia core complex proteins was intact because, although total levels of FANCD2 were reduced in these cells, both FANCD2-S and FANCD2-L were present in small amounts even before complementation. That is, the capacity for monoubiquitination (a function that depends on all eight Fanconi anemia core proteins) existed, although the total amount of FANCD2 was low. We showed that the total FANCD2 level was inadequate to protect cells against MMC-induced chromosomal breakage by observing that ectopic expression of FANCD2 complemented MMC hypersensitivity.

Table 3. Genomic losses identified by whole genomic oligonucleotide array CGH

Cell line	Chromosome band	DNA sequence coordinates*	Genes present[†]
OV-HR2	1q32.1	199173282-199267956	*PPP1R12B*
	6p21.3	31479350-31479458	*MICA*
	9p22.3	14791818-14839785	*FREM1*
	22q11.1	18623365-18623937	*ACTBL1/POTE14*
	14q11.2	19385491-19491463	*HLA-DRB*
	22q13.1	37686171-37712360	*GVD*[‡]
OV-CA4	6p21.3	32593507-32593134	*HLA-DRB5*
	8q22.3	100094670-100094751	*VPS13B*
	11p15.2-14.3	1122646230-22646457	*GAS2*
	5q13.2	69690000-69990000	*GVD*
	8p23.1	7230000-7890000	*GVD*
	14q11.2	18750000-19470000	*GVD*
	15q11.2	18330000-20250000	*GVD*

*Breakpoint interval defined by whole-genome oligonucleotide array CGH.
[†]Only characterized genes are listed.
[‡]Regions of loss listed as a copy number variant in the Database of Genomic Variants (GVD; Toronto; http://projects.tcag.ca/variation).

Complementation by *FANCD2* cDNA would not have occurred if any one of the core complex proteins was deficient.

We sought to discern the underlying cause of reduced FANCD2 protein expression. Although *FANCD2* maps to 3p25.3, a chromosome region frequently lost in both sporadic human ovarian carcinomas (2) and some cases of familial ovarian cancer (37), in this series we found no evidence of *FANCD2* loss in the epithelial cells with low FANCD2 levels. Sequencing of *FANCD2* cDNA from these samples revealed no mutation that could account for the low levels of protein. We also found no evidence of hypermethylation in promoter regions of any of the Fanconi anemia genes, including *FANCD2* (Supplementary Fig. S1), nor polymorphisms in the promoter region that distinguished low FANCD2 samples from normal FANCD2 samples. Finally, we found no consistent differences in mRNA expression of two proliferation markers, *PCNA* and *CCND1* (cyclin D1), in the OSE tested (Supplementary Fig. S2), and therefore, we suspect that substantial differences in replicative rates do not account for differences in FANCD2 levels or MMC responses observed, although this notion will require further study using more direct methods in a larger series.

Our results implicate FANCD2 dysregulation in ovarian carcinogenesis and show that this abnormality may be limited to specific epithelial cell types. That is, in contrast to OSE cells, *FANCD2* mRNA and protein levels in peripheral blood lymphocytes from the same patients were not reduced when compared with normal controls (Figs. 1*C* and *D* and 2*A*). Although we have ruled out loss of p53 function as an explanation (Fig. 1*B*), we have not yet discovered a molecular mechanism for suppression of *FANCD2* gene expression in these ovarian cells. That both protein and mRNA were suppressed in these cells but not in lymphocytes and that no mutations in *FANCD2* were detected suggest several potential mechanisms. First, mutations or polymorphisms in *cis*-acting tissue-specific and/or hormonally responsive *FANCD2* control regions (outside the promoter regions studied) might exist in these OSE cells. Second, tissue-specific inactivating mutations of FANCD2 transactivating factors might exist as well. Further studies are clearly warranted to clarify a role for FANCD2, as well as identify factors that specifically control its expression, in ovarian epithelial cells.

It is also unclear how reduced FANCD2 levels might drive malignant transformation of OSE cells. Theoretically, loss of FANCD2 function in these cells might provide them with a unique survival advantage. We believe this to be unlikely because loss of other Fanconi anemia alleles results in a proapoptotic phenotype in the ground state (38). Consequently, before FANCD2 suppression can be tolerated by a cell population, early somatic mutations would probably have to occur first to protect the cells from the apoptotic consequences of FANCD2 loss. Such changes are known to occur in neoplastic hematopoietic cells (39) and argue in favor of a general model of early clonal adaptation in neoplastic Fanconi anemia cells (40).

Not all ovarian cancer predisposition genes have been identified, so mutation screening of *BRCA1* and *BRCA2* cannot accurately identify at-risk patients who are members of ovarian cancer families. Although the data presented here derive from a small series, they indicate that, by using cross-linking agent sensitivity testing, there is a high prevalence of genetically unstable epithelial cells in women from cancer families. With some practical modifications using minimally invasive methods or testing more readily accessible epithelial tissues (i.e., uterine cervix), the application of this assay as a screening tool may represent a way of distinguishing women at high risk from their female relatives who are not.

References

1. Okamura H, Katabuchi H. Pathophysiological dynamics of human ovarian surface epithelial cells in epithelial ovarian carcinogenesis. Int Rev Cytol 2005; 242:1–54.

2. Mitelman F, Mertens F, Johansson B. Prevalence estimates of recurrent balanced cytogenetic aberrations and gene fusions in unselected patients with neoplastic disorders. Genes Chromosomes Cancer 2005;43:350–66.

3. Slamon DJ, Godolphin W, Jones LA, et al. Studies of the HER-2/*neu* proto-oncogene in human breast and ovarian cancer. Science 1989;244:707–12.

4. Enomoto T, Weghorst CM, Inoue M, Tanizawa O, Rice JM. K-ras activation occurs frequently in mucinous adenocarcinomas and rarely in other common epithelial tumors of the human ovary. Am J Pathol 1991;139:777–85.

5. Tashiro H, Miyazaki K, Okamura H, Iwai A, Fukumoto M. c-*myc* over-expression in human primary ovarian tumours: its relevance to tumour progression. Int J Cancer 1992;50:828–33.

6. Bellacosa A, de Feo D, Godwin AK, et al. Molecular alterations of the AKT2 oncogene in ovarian and breast carcinomas. Int J Cancer 1995;64:280–5.

7. Shayesteh L, Lu Y, Kuo WL, et al. PIK3CA is implicated as an oncogene in ovarian cancer. Nat Genet 1999;21: 99–102.

8. Fukasawa K, Choi T, Kuriyama R, Rulong S, Vande Woude GF. Abnormal centrosome amplification in the absence of p53. Science 1996;271:1744–7.

9. Obata K, Morland SJ, Watson RH, et al. Frequent PTEN/MMAC mutations in endometrioid but not serous or mucinous epithelial ovarian tumors. Cancer Res 1998;58:2095–7.

10. Yu Y, Xu F, Peng H, et al. NOEY2 (ARHI), an imprinted putative tumor suppressor gene in ovarian and breast carcinomas. Proc Natl Acad Sci U S A 1999;96:214–9.

11. Schorge JO, Miller YB, Qi LJ, et al. Genetic alterations of the WT1 gene in papillary serous carcinoma of the peritoneum. Gynecol Oncol 2000;76:369–72.

12. McCoy ML, Mueller CR, Roskelley CD. The role of the breast cancer susceptibility gene 1 (BRCA1) in sporadic epithelial ovarian cancer. Reprod Biol Endocrinol 2003; 1:72.

13. Meetei AR, Levitus M, Xue Y, et al. X-linked inheritance of Fanconi anemia complementation group B. Nat Genet 2004;36:1219–24.

14. Levitus M, Waisfisz Q, Godthelp BC, et al. The DNA helicase BRIP1 is defective in Fanconi anemia complementation group J. Nat Genet 2005;37:934–5.

15. Levran O, Attwooll C, Henry RT, et al. The BRCA1-interacting helicase BRIP1 is deficient in Fanconi anemia. Nat Genet 2005;37:931–3.

16. Garcia-Higuera I, Taniguchi T, Ganesan S, et al. Interaction of the Fanconi anemia proteins and BRCA1 in a common pathway. Mol Cell 2001;7:249–62.

17. Taniguchi T, Garcia-Higuera I, Andreassen PR, Gregory RC, Grompe M, D'Andrea AD. S-phase-specific interaction of the Fanconi anemia protein, FANCD2, with BRCA1 and RAD51. Blood 2002;100:2414–20.

18. Hussain S, Wilson JB, Medhurst AL, et al. Direct interaction of FANCD2 with BRCA2 in DNA damage response pathways. Hum Mol Genet 2004;13:1241–8.

19. Shimamura A, de Oca RM, Svenson JL, et al. A novel diagnostic screen for defects in the Fanconi anemia pathway. Blood 2002;100:4649–54.

20. Howlett NG, Taniguchi T, Olson S, et al. Biallelic inactivation of BRCA2 in Fanconi anemia. Science 2002; 297:606–9.

21. Houghtaling S, Timmers C, Noll M, et al. Epithelial cancer in Fanconi anemia complementation group D2 (Fancd2) knockout mice. Genes Dev 2003;17:2021–35.

22. Taniguchi T, Tischkowitz M, Ameziane N, et al. Disruption of the Fanconi anemia-BRCA pathway in cisplatin-sensitive ovarian tumors. Nature Med 2003;9: 568–74.

23. U.S. Preventive Services Task Force recommendations. Summaries for patients. Genetic risk assessment and BRCA mutation testing for breast and ovarian cancer susceptibility. Ann Intern Med 2005;143:I47.

24. Saito H, Hammond AT, Moses RE. Hypersensitivity to oxygen is a uniform and secondary defect in Fanconi anemia cells. Mutat Res 1993;294:255–62.

25. Williams DA, Rosenblatt MF, Beier DR, Cone RD. Generation of murine stromal cell lines supporting hematopoietic stem cell proliferation by use of recombinant retrovirus vectors encoding simian virus 40 large T antigen. Mol Cell Biol 1988;8:3864–71.

26. Naf D, Kupfer GM, Suliman A, Lambert K, D'Andrea AD. Functional activity of the Fanconi anemia protein FAA requires FAC binding and nuclear localization. Mol Cell Biol 1998;18:5952–60.

27. Kuang Y, Garcia-Higuera I, Moran A, Mondoux M, Digweed M, D'Andrea AD. Carboxy terminal region of the Fanconi anemia protein, FANCG/XRCC9, is required for functional activity. Blood 2000;96:1625–32.

28. Pang Q, Keeble W, Christianson TA, Faulkner GR, Bagby GC. FANCC interacts with Hsp70 to protect hematopoietic cells from IFN-γ/TNF-α-mediated cytotoxicity. EMBO 2001;20:4478–89.

29. Livak KJ, Schmittgen TD. Analysis of relative gene expression data using real-time quantitative PCR and the $2(-\Delta\Delta C(T))$ method. Methods 2001;25:402–8.

30. Selzer RR, Richmond TA, Pofahl NJ, et al. Analysis of chromosome breakpoints in neuroblastoma at sub-kilobase resolution using fine-tiling oligonucleotide array CGH. Genes Chromosomes Cancer 2005;44:305–19.

31. Olshen AB, Venkatraman ES, Lucito R, Wigler M. Circular binary segmentation for the analysis of array-based DNA copy number data. Biostatistics 2004; 5:557–72.

32. Nygren AO, Ameziane N, Duarte HM, et al. Methylation-specific MLPA (MS-MLPA): simultaneous detection of CpG methylation and copy number changes of up to 40 sequences. Nucleic Acids Res 2005;33:e128.

33. Schouten JP, McElgunn CJ, Waaijer R, Zwijnenburg D, Diepvens F, Pals G. Relative quantification of 40 nucleic acid sequences by multiplex ligation-dependent probe amplification. Nucleic Acids Res 2002;30:e57.

34. Pestell K, Medlow C, Titley J, Kelland L, Walton M. Characterisation of the P53 status, Bcl-2 expression, and radiation and platinum drug sensitivity of a panel of human ovarian cancer cell lines. Int J Cancer 1998;77: 913–8.

35. van Beusechem V, van den Doel P, Grill J, Pinedo H, Gerritsen W. Conditionally replicative adenovirus expressing p53 exhibits enhanced oncolytic potency. Cancer Res 2002;62:6165–71.

36. Offit K. Clinical cancer genetics: risk counseling and management. New York: Wiley-Liss, Inc.; 1998. p. 115–24.

37. Zhang GL, Xu KL. Loss of heterozygosity at chromosome 3p in epithelial ovarian cancer in China. Int J Gynecol Cancer 2002;12:198–201.

38. Bagby GC, Jr. Genetic basis of Fanconi anemia. Curr Opin Hematol 2003;10:68–76.

39. Lensch MW, Rathbun RK, Olson SB, Jones GR, Bagby GC, Jr. Selective pressure as an essential force in molecular evolution of myeloid leukemic clones: a view from the window of Fanconi anemia. Leukemia 1999;13:1784–9.

40. Bagby GC, Olson SB. Cisplatin and the sensitive cell. Nat Med 2003;9:513–4.

AACR American Association
for Cancer Research

Cytogenetic Instability in Ovarian Epithelial Cells from Women at Risk of Ovarian Cancer

Tanja Pejovic, Jane E. Yates, Hong Y. Liu, et al.

Updated version	Access the most recent version of this article at: http://cancerres.aacrjournals.org/content/66/18/9017
Supplementary Material	Access the most recent supplemental material at: http://cancerres.aacrjournals.org/content/suppl/2006/09/19/66.18.9017.DC1

Cited articles	This article cites 39 articles, 14 of which you can access for free at: http://cancerres.aacrjournals.org/content/66/18/9017.full#ref-list-1
Citing articles	This article has been cited by 7 HighWire-hosted articles. Access the articles at: http://cancerres.aacrjournals.org/content/66/18/9017.full#related-urls

E-mail alerts	Sign up to receive free email-alerts related to this article or journal.
Reprints and Subscriptions	To order reprints of this article or to subscribe to the journal, contact the AACR Publications Department at pubs@aacr.org.
Permissions	To request permission to re-use all or part of this article, use this link http://cancerres.aacrjournals.org/content/66/18/9017. Click on "Request Permissions" which will take you to the Copyright Clearance Center's (CCC) Rightslink site.